

Title	Quasi-elastic neutron scattering studies on fast dynamics of water molecules in tetra- n - butylammonium bromide semiclathrate hydrate
Author(s)	Shimada, Jin; Tani, Atsushi; Yamada, Takeshi et al.
Citation	Applied Physics Letters. 2023, 123(4), p. 50
Version Type	VoR
URL	https://hdl.handle.net/11094/92418
rights	This article may be downloaded for personal use only. Any other use requires prior permission of the author and AIP Publishing. This article appeared in Jin Shimada, Takeshi Yamada, Takeshi Sugahara, Takayuki Hirai, and Takuo Okuchi, "Quasi-elastic neutron scattering studies on fast dynamics of water molecules in tetra-n-butylammonium bromide semiclathrate hydrate", Applied Physics Letters 123, 50 (2023) and may be found at https://doi.org/10.1063/5.0157560 .
Note	









Osaka University Knowledge Archive : OUKA

<https://ir.library.osaka-u.ac.jp/>

Osaka University

RESEARCH ARTICLE | JULY 26 2023

Quasi-elastic neutron scattering studies on fast dynamics of water molecules in tetra-*n*-butylammonium bromide semiclathrate hydrate

Jin Shimada ; Atsushi Tani  ; Takeshi Yamada ; Takeshi Sugahara  ; Takayuki Hirai ; Takuo Okuchi 

 Check for updates

Appl. Phys. Lett. 123, 044104 (2023)

<https://doi.org/10.1063/5.0157560>



View Online

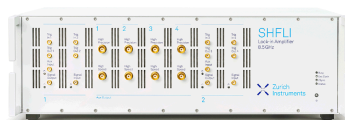


Export Citation

CrossMark

500 kHz or 8.5 GHz?
And all the ranges in between.

Lock-in Amplifiers for your periodic signal measurements



Find out more



Quasi-elastic neutron scattering studies on fast dynamics of water molecules in tetra-*n*-butylammonium bromide semiclathrate hydrate

Cite as: Appl. Phys. Lett. **123**, 044104 (2023); doi: 10.1063/5.0157560

Submitted: 9 May 2023 · Accepted: 6 July 2023 ·

Published Online: 26 July 2023









View Online



Export Citation



CrossMark

Jin Shimada,^{1,2,3}  Atsushi Tani,^{4,5,a)}  Takeshi Yamada,⁶  Takeshi Sugahara,^{1,2,a)}  Takayuki Hirai,^{1,2} 
and Takuo Okuchi⁷ 

AFFILIATIONS

¹Division of Chemical Engineering, Department of Materials Engineering Science, Graduate School of Engineering Science, Osaka University, 1-3 Machikaneyama, Toyonaka, Osaka 560-8531, Japan

²Division of Energy and Photochemical Engineering, Research Center for Solar Energy Chemistry, Graduate School of Engineering Science, Osaka University, 1-3 Machikaneyama, Toyonaka, Osaka 560-8531, Japan

³Research Fellow of Japan Society for the Promotion of Science, 5-3-1 Kojimachi, Chiyoda-ku, Tokyo 102-0083, Japan

⁴Department of Human Environmental Science, Graduate School of Human Development and Environment, Kobe University, 3-11 Tsurukabuto, Nada, Kobe, Hyogo 657-8501, Japan

⁵Division of Terahertz Molecular Chemistry Laboratory, Molecular Photoscience Research Center, Kobe University, 1-1 Rokkodai, Nada, Kobe, Hyogo 657-8501, Japan

⁶Neutron Science and Technology Center, Comprehensive Research Organization for Science and Society, 162-1 Shirakata, Tokai, Naka, Ibaraki 319-1106, Japan

⁷Institute for Integrated Radiation and Nuclear Science, Kyoto University, 2 Asashiro-Nishi, Kumatori, Osaka 590-0494, Japan

^{a)}Authors to whom correspondence should be addressed: tani@carp.kobe-u.ac.jp and sugahara@cheng.es.osaka-u.ac.jp

ABSTRACT

The dynamics of the water molecules in tetra-*n*-butyl-*d*36-ammonium bromide semiclathrate hydrate was investigated by quasi-elastic neutron scattering (QENS). The QENS results clearly revealed a fast reorientation motion of water molecules in the temperature range of 212–278 K. The mean jump distance of hydrogen atoms was within 1.5–2.0 Å. The relaxation time of water reorientation was estimated to be 100–410 ps with an activation energy of 10.2 ± 5.8 kJ·mol⁻¹. The activation energy was in good agreement with the cleavage energy of hydrogen bonds. Such a short relaxation time of water reorientation is possibly due to strong interaction between a bromide anion and its surrounding water molecules (similar to so-called negative hydration), which suggests a unique strategy for designing efficient, safe, and inexpensive proton conductors having the framework of semiclathrate hydrates.

Published under an exclusive license by AIP Publishing. <https://doi.org/10.1063/5.0157560>

Proton conduction phenomenon in ices has attracted many researchers due to unusually active dynamic behaviors of water molecules in the crystalline compounds. Remarkably, it is known that the proton conductivity in ice I_h (10^{-6} – 10^{-7} S·cm⁻¹) is higher than in liquid water,^{1–4} and the conduction mechanism in crystalline ices is considered to be fundamentally different from liquid water.^{5–8} Clathrate hydrate also shows proton conduction phenomenon,^{9–12} in which hydrogen-bonded networks of water molecules form the crystal framework, as in the case of ices. Various properties of clathrate hydrates

can be designed by selecting guest species to be enclathrated into hydrate cages. In fact, even ionic guest species are allowed to be enclathrated, which enhances the proton conduction; clathrate hydrates formed with perchloric acid or hexafluorophosphoric acid, which supplies the large number of protons, are known as the proton conductors with a conductivity (about 10^{-3} or 10^{-1} S·cm⁻¹ at 273 K,^{13,14} respectively) higher than ices. However, these aqueous solutions with strongly acidity are difficult to handle and limited in their applications. Therefore, establishing a strategy to design well-proton-

conducting clathrate hydrate from easily handled guest species is an important task for its future and practical applications.

As a way to solve the task, we have focused on semiclathrate hydrates (or ionic clathrate hydrates). Semiclathrate hydrate is a crystalline inclusion compound, in which quaternary ammonium or phosphonium cation is incorporated into hydrate cages. The counter anions take part in the hydrogen-bonded networks as part of the host substance with water molecules.^{15,16} Among easily handled semiclathrate hydrates, tetra-*n*-butylammonium bromide (TBAB) semiclathrate hydrate^{15,17,18} has the relatively high electrical conductivity.^{19,20} Therefore, semiclathrate hydrates have been considered to be one of the promising candidates for highly conductive solid electrolytes.^{19–21} Recently, we reinforced this consideration by revealing that the proton was the charge carrier, which induces the proton conductivity of $4.1 \times 10^{-6} \text{ S}\cdot\text{cm}^{-1}$ at 273 K, in the case of single-crystalline TBAB semiclathrate hydrate.²⁰

Though TBAB semiclathrate hydrate has a proton conductivity^{19,20} higher than that of ices or general clathrate hydrates (so-called gas hydrates, consisting of nonionic molecules such as CH_4 or CO_2 ¹²), the relaxation time of water molecules in TBAB semiclathrate hydrate obtained by a nuclear magnetic resonance (NMR) was observed to be almost the same as that of ices or general clathrate hydrates.²² This apparent discrepancy suggests that a hidden mechanism of proton transfer would have enhanced the conductivity in TBAB semiclathrate hydrate, since the number of protons in it may not be so much increased compared with the general clathrate hydrates. To find the answer, it is necessary to analyze the water reorientation motion in a frequency window wider than that measurable by NMR. This is because the mechanism of the proton transfer in the clathrate hydrates or ices reflects the nature of water dynamics, especially of molecular reorientation motion.^{1–11,20,22–24}

In the present study, to reveal the role of fast water dynamics for inducing a conductivity higher than ices or clathrate hydrates, we conducted quasi-elastic neutron scattering (QENS) measurement of the TBAB semiclathrate hydrate. QENS (the measurable time window is from picosecond to nanosecond) allows us to investigate the molecular dynamics much faster than that of NMR (nanosecond to microsecond). In the previous QENS studies on the water dynamics in clathrate hydrates, Desmedt *et al.* reported the reorientation motion of 700 ps at 220 K in the fast-proton-conducting perchloric acid clathrate hydrate.¹⁰ Occurrence of the long-range proton diffusion, accompanied by the reorientation motion, has been also reported in some other types of clathrate hydrate and ice by QENS, where the water dynamics in a timescale from picosecond to nanosecond orders have been observed.^{9–11,25} Nevertheless, there is no report on QENS results of TBAB semiclathrate hydrate.

The large difference of incoherent neutron scattering cross section between a hydrogen and a deuterium makes it possible to observe the dynamics of the water molecules selectively; therefore, perdeuterated tetra-*n*-butyl-*d*36-ammonium bromide semiclathrate hydrate (*d*-TBAB-26H₂O) was used. *d*-TBAB (99.5 at. %) was obtained from C/D/N Isotopes Inc. *d*-TBAB-26H₂O was carefully prepared at 285.0 K to prevent the formation of metastable crystals, i.e., TBAB-38H₂O.¹⁶ Obtained crystal was quenched and powdered at a liquid nitrogen temperature. The sample was wrapped in aluminum foil ($\sim 10 \mu\text{m}$ thick) to maintain a thin-walled annular geometry in bulk. The foil-wrapped sample was placed in an aluminum cell (a thickness of 0.25 mm and an inner diameter of 14.0 mm). The cell was mechanically sealed with an

indium wire under dry helium atmosphere (purity: 0.999999) equipped at low-temperature room kept at 263 K. The sample cell was stored in a dry-shipper at 77 K just before the measurement.

The QENS measurements were carried out using the near-backscattering spectrometer (DNA) at Materials and Life Science Experimental Facility (MLF), Japan Proton Accelerator Research Complex (J-PARC) with high signal-to-noise ratio and high energy resolution.²⁶ The energy resolution was 3.6 μeV using the Si(111) analyzer. The measured momentum transfer (Q) and energy transfer (ΔE) ranges were $0.1 < Q < 1.9 \text{ \AA}^{-1}$ and $-40 < \Delta E < 100 \mu\text{eV}$, respectively. The cell was quickly mounted on a sample stick, and then the stick was inserted in a top-loading-type cryo-furnace equipped at the DNA which was controlled at 100 K to prevent dissociation of the sample. No condensation of bulk water was confirmed by temperature dependence of the elastic intensity, as shown in supplementary material Fig. S1. The QENS was measured at 212, 232, 252, 272, and 278 K. The resolution function, $R(Q, \omega)$, was measured at 8 K, where we assumed that all molecular dynamics were frozen. A typical measurement duration was around 4 h at 700 kW proton beam power. An empty cell was measured at 300 K to subtract background from the container.

The obtained Q - ΔE maps are shown in Fig. 1(a). A Bragg peak was observed at $Q = 0.6 \text{ \AA}^{-1}$ at elastic position ($\Delta E = 0$) in all measured data. The profile of the elastic intensity was shown in supplementary material Fig. S2. The peak position agreed with the literature value (0.6 \AA^{-1}) of TBAB semiclathrate hydrate (TBAB-26H₂O: tetragonal structure, space group: $P4/mmm$),^{27,28} which indicates the existence of *d*-TBAB-26H₂O in the whole range of measurement temperature. The intensity corresponding to QENS was observed in the inelastic region at temperatures above 212 K. The QENS intensity increased and broadened with an increase in temperature. The representative QENS profiles ($S(Q, E)$ at $Q = 0.875 \text{ \AA}^{-1}$) are also shown in Fig. 1(b). The narrow elastic and the broad quasi-elastic components were observed. Since the ratio of incoherent scattering cross section of water is 87% to the total scattering cross section of *d*-TBAB-26H₂O, the observed intensity corresponds to the hydrogen of water in *d*-TBAB-26H₂O and reflects the dynamics of water. The elastic and quasi-elastic components derived from immobile and mobile hydrogen, respectively. The QENS profile was deconvoluted into elastic and quasi-elastic components using the following equation:^{9–11,29}

$$S(Q, \omega) = [A_D(Q)\delta(\omega) + A_L(Q)L(\Gamma_L, \omega)] \otimes R(Q, \omega) + \text{BG}(Q). \quad (1)$$

The elastic component and the quasi-elastic component were represented by delta function (δ) and Lorentzian function (L), respectively. The A_D and A_L are the coefficients of delta and Lorentzian functions, respectively. Γ_L is half width at half maximum of Lorentzian function. BG represents the background. The fitting results are also shown in Fig. 1(b).

Figure 2 shows the half width at half maximum (Γ_L) of the Lorentzian function [$L(\Gamma_L, \omega)$] plotted as a function of Q . The linewidth was independent of Q . This result implies that the mobile hydrogen atoms are localized in a limited space.

The relaxation time (τ) of hydrogen dynamics was estimated from the linewidth (Fig. 2) using the following equation:

$$\tau = \frac{1}{2\pi\Gamma_L \times (2.418 \times 10^{11})}. \quad (2)$$

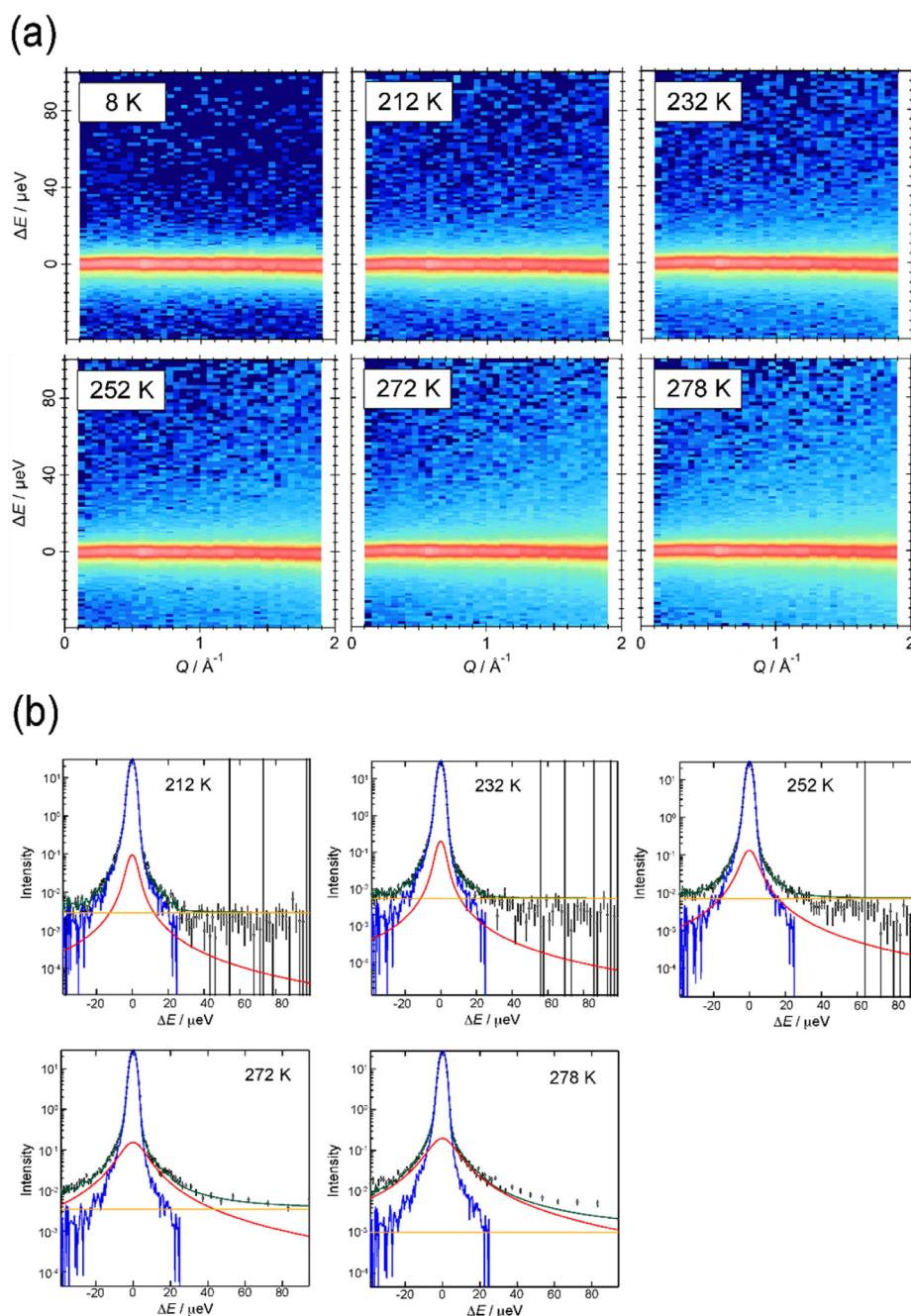


FIG. 1. (a) Q - ΔE maps of d -TBAB·26H₂O obtained by QENS measurement. The red-colored region means the high scattering intensity. (b) The representative Q -sliced QENS profiles at $Q = 0.875 \pm 0.075 \text{ \AA}^{-1}$ measured at 212, 232, 252, 272, and 278 K. Fitting results were shown as fitted function (green), delta function (blue), Lorentzian function (red), and background (orange).

The obtained relaxation time (Fig. 3) was 100–410 ps at 278–212 K. The estimated activation energy E_a was $10.2 \pm 5.8 \text{ kJ}\cdot\text{mol}^{-1}$, which is close to the cleavage energy of hydrogen bonds between water molecules.²⁴

An elastic incoherent structure factor (EISF) was expressed as Eq. (3) and shown in Fig. 4(a),

$$EISF = \frac{A_D}{A_D + A_L}. \quad (3)$$

The fitting curves of EISF were drawn by using jumping model between two sites,²⁵ which showed the highest accuracy among 2–4 sites,

$$EISF(Q) = f + (1 - f) \left[\frac{1}{2} (1 + j_0(Qd)) \right], \quad (4)$$

where the symbols f , j_0 , and d stand for the fraction of immobile hydrogen, Bessel function of zeroth order, and jump distance between

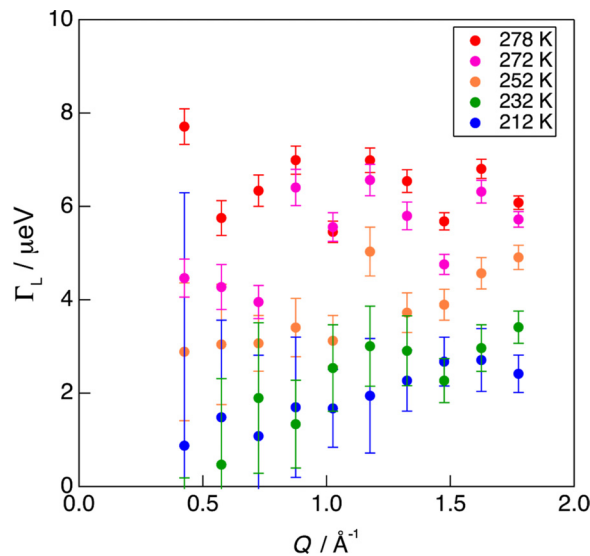


FIG. 2. The half width at half maximum (Γ_L) of the Lorentzian function [$L(Q, \omega)$] plotted as a function of Q . The Γ_L was independent of Q . Such trend implies that the mobile space of the hydrogen atoms is limited.

two sites, respectively. Supplementary material Figs. S3 and S4 show the fitting results of EISF with various d values from 1.0 to 2.8 Å. The EISF results fitted well with the mean jump distance between 1.5 and 2.0 Å. As the representative data, the fitting results ($d = 1.8$ Å) of EISF were shown in Fig. 4(a). The obtained mean jump distance (1.5–2.0 Å) agreed well with the reorientation distance of hydrogen atoms around the oxygen atom of water molecules (1.5–1.8 Å),^{9,25} whereas it was different from the jump distances of proton transfer and long-range proton diffusion, which should be about 1.0 Å (H···O distance) and about 2.8 Å (O···O distance), respectively.

The mechanism of the proton transfer in the clathrate hydrates or ices is related to the water dynamics, especially molecular reorientation motion.^{1–11,20} At Bjerrum defects, proton transfer is temporarily suspended, where the reorientation of the water molecules (or hydronium ions) is necessary to restart the transfer. In other words, the

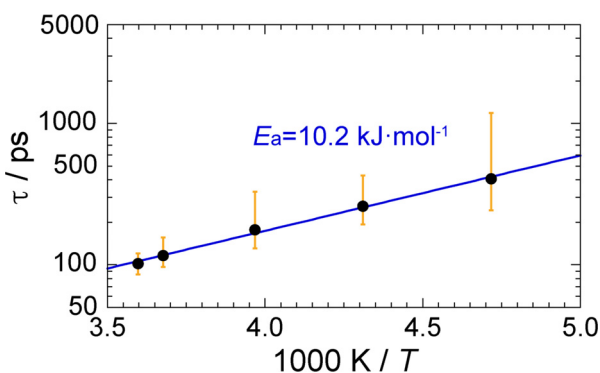


FIG. 3. Arrhenius plots of the relaxation time (τ) of hydrogen dynamics observed by QENS measurement. The estimated activation energy was 10.2 ± 5.8 kJ·mol⁻¹, which showed good agreement with the cleavage energy of hydrogen bonds.

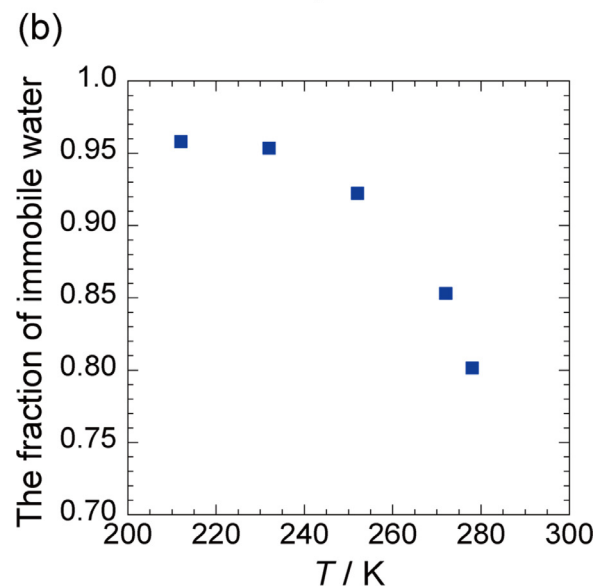
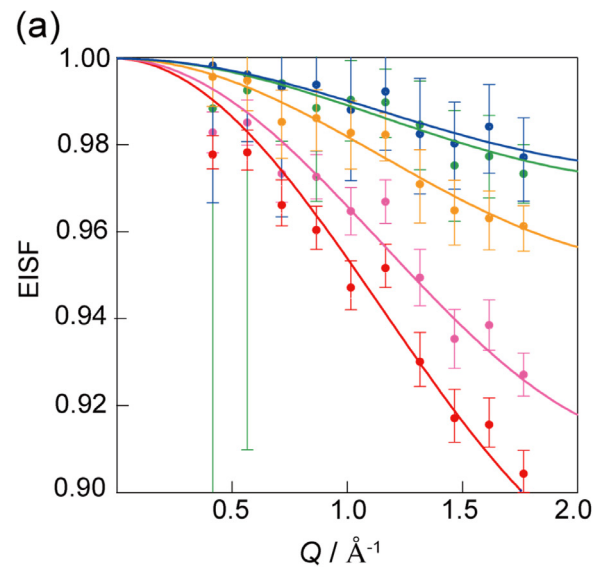


FIG. 4. (a) EISF results plotted as Q . The fitting curves were calculated using Eq. (4) with $d = 1.8$ Å. The colors reflect the temperatures, such as 212 K (blue), 232 K (green), 252 K (orange), 272 K (pink), and 278 K (red). (b) The immobile fraction in Eq. (4) corresponding to immobile water in d -TBAB-26H₂O. The fraction depended strongly on the temperatures.

reorientation of water molecules so as to alleviate the defects is a rate-limiting step of proton conduction.²³ The relaxation times obtained by QENS in TBAB-26H₂O were much shorter than the relaxation time (approximately $0.5 \mu\text{s}$ ³⁰ or $12 \mu\text{s}$ ²⁰ at 273 K) obtained by NMR measurement, although both the activation energies of QENS and NMR were similar to the cleavage energy of hydrogen bonds (about $14 \text{ kJ}\cdot\text{mol}^{-1}$)²⁴ rather than proton (ionic defect) generation energy (approximately $70 \text{ kJ}\cdot\text{mol}^{-1}$).^{31,32} In fact, such the reorientation motion of water with hundreds of picosecond order has been universally observed in the other type of ionic clathrate hydrate

($\text{HClO}_4 \cdot 5.5\text{H}_2\text{O}$),¹⁰ which is a well-known ionic conductor. The jump distance, the relaxation time, and the activation energy of $\text{HClO}_4 \cdot 5.5\text{H}_2\text{O}$ are 1.45 Å, 700 ± 100 ps, and 17.4 ± 1.5 kJ·mol⁻¹ at 220 K, respectively. The results obtained in the present study are similar to these values in $\text{HClO}_4 \cdot 5.5\text{H}_2\text{O}$, suggesting that the semiclathrate hydrate can be as useful as the ionic clathrate hydrate.

Figure 4(b) shows the f in Eq. (4) corresponding to immobile water molecules. The fraction of immobile water molecules depended strongly on the temperatures. Around 220 K, the ratio of mobile water molecules was only 4%. Near the dissociation temperature of d -TBAB·26H₂O, the mobile water population increased to 18%. This ratio of 18% means that approximately five water molecules per 1 unit (d -TBAB·26H₂O) near the dissociation temperatures are in motion, whereas the ratio of 4% around 220 K corresponds to a single water molecule per 1 unit. The trend of its temperature dependence is reasonable to qualitatively explain the temperature dependence of the electrical conductivity in TBAB·26H₂O at 270–286 K.²⁰ The five water molecules are close to the number of water molecules coordinating around the bromide anion. Such results mean that the bromide anion activates the reorientation motion of the water molecules locally in TBAB·26H₂O, which resembles a negative hydration around bromide anion in the aqueous solution. Considering the results of NMR measurement, the other water molecules rotate more slowly (Fig. 5).

The features of hydrogen dynamics in d -TBAB·26H₂O interpreted from the perspectives of jump distance, activation energy, relaxation time, and ratio of water molecules contributing QENS can be summarized as follows: (1) the hydrogen is locally transferred; (2) the hydrogen jump distance between two sites is within 1.5–2.0 Å; (3) the activation energy is 10.2 ± 5.8 kJ·mol⁻¹, which is close to the cleavage energy of hydrogen bonds; (4) the relaxation time is 100–410 ps; and (5) the ratio of water molecules contributing to QENS is 4%–18%. These results revealed that the signals observed by QENS measurement are derived from the fast (hundreds of ps order) reorientation motion of the water molecules around bromide anions in TBAB·26H₂O. The μ s-order reorientation motion measurable by NMR is detected in the general clathrate hydrate and ice as well as TBAB·26H₂O. Unlike the μ s-order reorientation motion obtained by

NMR, the hundreds-of-ps-order reorientation motion obtained in TBAB·26H₂O by QENS could make the proton transfer more smoothly in the region around bromide ion. As mentioned earlier, proton transfer is temporarily suspended at Bjerrum defects. To restart the proton transfer, that is, to alleviate the defects, the reorientation motion of water molecules is inevitably required. The fast water reorientation motion obtained in TBAB·26H₂O by QENS would contribute to shortening the residence time of proton at the Bjerrum defects accidentally formed around bromide ion. This would be the reason why the TBAB·26H₂O had a bulk proton conductivity higher than the general clathrate hydrates and ices.

In summary, the reorientation motion on the order of some hundreds of picoseconds was observed in TBAB semiclathrate hydrate (d -TBAB·26H₂O) by QENS measurement. Such relaxation times obtained by QENS are much shorter than that of the order of microseconds previously obtained by NMR for the same medium. The fast water reorientation should be caused by the negative hydration-like behavior of the water molecules surrounding bromide anion. Why TBAB semiclathrate hydrate exhibits the high proton conductivity would be originated from this fast water reorientation motion around bromide ion observed by QENS. The results provided the tips to improve the conductivity of semiclathrate hydrates and suggested the possibility of unconventional applications such as solid-state electrolytes.

See the supplementary material for experimental data including an elastic intensity of d -TBAB·26H₂O and the fitting results of EISF with various d values.

This work was supported by JSPS KAKENHI Grant-in-Aid for JSPS Fellows (Nos. JP21J20788 and JP22KJ2069 for J.S.) and Grand-in-Aid for Scientific Research (Nos. JP17H06456 for A.T., JP22K05050 for T.S., and JP21H04519 for T.O.). The QENS experiment at the Materials and Life Science Experimental Facility of the J-PARC was performed under a user program (Proposal No. 2021B0086).

AUTHOR DECLARATIONS

Conflict of Interest

The authors have no conflicts to disclose.

Author Contributions

Jin Shimada: Conceptualization (equal); Data curation (equal); Formal analysis (equal); Funding acquisition (equal); Investigation (equal); Validation (equal); Writing – original draft (equal); Writing – review & editing (equal). **Atsushi Tani:** Conceptualization (equal); Funding acquisition (equal); Investigation (equal); Project administration (equal); Supervision (equal); Validation (equal); Writing – review & editing (equal). **Takeshi Yamada:** Data curation (equal); Formal analysis (equal); Investigation (equal); Methodology (equal); Project administration (equal); Validation (equal); Writing – original draft (equal); Writing – review & editing (equal). **Takeshi Sugahara:** Funding acquisition (equal); Supervision (equal); Validation (equal); Writing – review & editing (equal). **Takayuki Hirai:** Supervision (equal); Writing – review & editing (equal). **Takuo Okuchi:** Funding acquisition (equal); Project administration (equal); Supervision (equal); Writing – review & editing (equal).

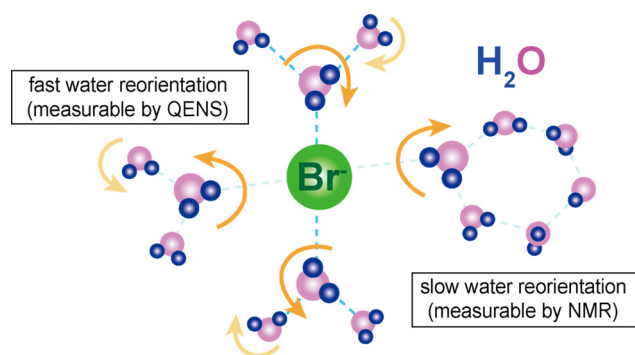


FIG. 5. Illustration of the dynamics of the water molecules around bromide anions (measurable by QENS) and the other water molecules (by NMR) in TBAB·26H₂O. The fast water reorientation around bromide anions represents the negative hydration-like region, whereas the slow water reorientation in the other water molecules stands for the rigid hydrogen-bonded region.

DATA AVAILABILITY

The data that support the findings of this study are available from the corresponding author upon reasonable request.

REFERENCES

- ¹H. Gränicher, C. Jaccard, P. Scherrer, and A. Steinemann, *Discuss. Faraday Soc.* **23**, 50 (1957).
- ²M. Eigen and L. De Maeyer, *Proc. R. Soc. Lond. A* **247**, 505 (1958).
- ³M. Eigen, *Angew. Chem., Int. Ed. Engl.* **3**, 1 (1964).
- ⁴J. W. Glen and J. G. Paren, *J. Glaciol.* **15**, 15 (1975).
- ⁵C. Jaccard, *Helv. Phys. Acta* **32**, 89 (1959).
- ⁶C. Jaccard, *Phys. Kondens. Mater.* **3**, 99 (1964).
- ⁷C. Jaccard, *Ann. N. Y. Acad. Sci.* **125**, 390 (2006).
- ⁸L. Onsager and M. Dupuis, "The electrical properties of ice," in *Electrolytes* edited by B. Pesce (Pergamon Press, Oxford, 1962).
- ⁹A. Desmedt, F. Stallmach, R. E. Lechner, and M. A. Gonzalez, *J. Chem. Phys.* **121**, 11916 (2004).
- ¹⁰A. Desmedt, R. E. Lechner, J.-C. Lassegues, F. Guillaume, D. Cavagnat, and J. Grondin, *Solid State Ionics* **252**, 19 (2013).
- ¹¹L. Bedouret, P. Judeinstein, J. Ollivier, J. Combet, and A. Desmedt, *J. Phys. Chem. B* **118**, 13357 (2014).
- ¹²L. A. Stern, S. Lu, R. Constable, W. L. Du Frane, and J. J. Roberts, *Geophys. Res. Lett.* **48**, e2021GL093475, <https://doi.org/10.1029/2021GL093475> (2021).
- ¹³J.-H. Cha, K. Shin, S. Choi, S. Lee, and H. Lee, *J. Phys. Chem. C* **112**(35), 13332 (2008).
- ¹⁴M. Cappadonia, A. A. Kornyshev, S. Krause, A. M. Kuznetsov, and U. Stimming, *J. Chem. Phys.* **101**, 7672–7682 (1994).
- ¹⁵W. Shimada, M. Shiro, H. Kondo, S. Takeya, H. Oyama, T. Ebinuma, and H. Narita, *Acta Crystallogr., Sect. C* **61**, o65 (2005).
- ¹⁶T. V. Rodionova, I. S. Terekhova, and A. Y. Manakov, *Energy Fuels* **36**(18), 10458 (2022).
- ¹⁷H. Machida, T. Sugahara, and I. Hirasawa, *CrystEngComm* **20**, 3328 (2018).
- ¹⁸H. Oyama, W. Shimada, T. Ebinuma, Y. Kamata, S. Takeya, T. Uchida, J. Nagao, and H. Narita, *Fluid Phase Equilib.* **234**, 131 (2005).
- ¹⁹Z. Borkowska, M. Opallo, A. Tymosiak-Zielinska, and P. Zoltowski, *Colloids Surf., A* **134**, 67 (1998).
- ²⁰J. Shimada, Y. Takaoka, T. Ueda, A. Tani, T. Sugahara, K. Tsunashima, H. Yamada, and T. Hirai, *Solid State Ionics, Solid State Ionics* **393**, 116188 (2023).
- ²¹N. Kuriyama, T. Sakai, H. Miyamura, A. Kato, and H. Ishikawa, *Solid State Ionics* **40**(41), 906 (1990).
- ²²E. D. Sloan and C. A. Koh, *Clathrate Hydrates of Natural Gases*, 3rd ed. (CRC Press, Boca Raton, FL, 2008).
- ²³D. H. Lee and H. Kang, *J. Phys. Chem. B* **125**, 8270 (2021).
- ²⁴N. Agmon, *Chem. Phys. Lett.* **244**, 456 (1995).
- ²⁵I. Presiado, J. Lal, E. Mamontov, A. I. Kolesnikov, and D. Huppert, *J. Phys. Chem. C* **115**(20), 10245 (2011).
- ²⁶K. Shibata, N. Takahashi, Y. Kawakita, M. Matsuura, T. Yamada, T. Tominaga, W. Kambara, M. Kobayashi, Y. Inamura, T. Nakatani, K. Nakajima, and M. Arai, *JPS Conf. Proc.* **8**, 036022 (2015).
- ²⁷M. Oshima, M. Kida, and J. Nagao, *J. Chem. Eng. Data* **61**(9), 3334 (2016).
- ²⁸T. V. Rodionova, V. Y. Komarov, G. V. Villevald, T. D. Karpova, N. V. Kuratieva, and A. Y. Manakov, *J. Phys. Chem. B* **117**(36), 10677 (2013).
- ²⁹T. Okuchi, N. Tomioka, N. Purevjav, and K. Shibata, *J. Appl. Crystallogr.* **51**, 1564 (2018).
- ³⁰S. Schildmann, A. Nowaczyk, B. Geil, C. Gainaru, and R. Böhmer, *J. Chem. Phys.* **130**, 104505 (2009).
- ³¹J. H. Bilgram and H. Gränicher, *Phys. Cond. Matter* **18**, 275 (1974).
- ³²I. Takei and N. Maeno, *J. Phys. Colloques* **48**, C1-121 (1987).